International Journal of Offshore and Polar Engineering (ISSN 1053-5381)

Vol. 18, No. 4, December 2008, pp. 254–262

Wave Scattering by an Infinite Straight-Line Array of Axisymmetric Floes

Luke G. Bennetts
Department of Mathematics and Statistics, University of Otago, Dunedin, New Zealand

Vernon A. Squire
Division of Sciences, University of Otago, Dunedin, New Zealand

The linear and time-harmonic problem of an infinite, equispaced, straight-line array of identical floes is considered. Under the asssumption of axisymmetry, the floes are permitted to vary in thickness through both their upper and lower surfaces. Further, a realistic draught may be incorporated. An approximation technique is implemented, which combines a variational principle and an association of the vertical motion to the mode that supports propagating waves. The resulting equations exist in the horizontal plane and are solved through the use of a Green's function in the free-surface domain and a Fourier expansion in the ice-covered domain. Numerical results are given for example problems that show the influence of the varying thickness and realistic draught.

INTRODUCTION

In the Arctic Basin and Southern Ocean the marginal ice zone (MIZ) comprises a vast number of individual ice floes, as well as regions of quasi-continuous ice cover. These floes are created on a seasonal basis through the freezing of surface water or from the fracture of the larger ice sheets, which is caused primarily through stresses induced by ocean waves. For this reason, the smaller, individual floes often form a barrier between the open ocean and the inner mass of ice. Waves that reach this inner mass will thus need to penetrate the boundary of smaller ice floes, and in doing so they will become attenuated. Occasionally, the band of individual floes and ice cakes may also detach from the rest of the ice pack to create a dissociated belt off the ice edge (Bauer and Martin, 1980).

The ice covering in the MIZ is relatively thin in comparison to its horizontal dimensions, and the standard method for modelling this situation is to use thin-plate theory (Timoshenko and Woinowsky-Krieger, 1959). In this context, the motions of the fluid-ice system, caused by ocean waves, manifest as flexural-gravity waves that travel at the interface between the 2 media. When forced by an incident ocean wave, as well as exhibiting the so-called rigid-body modes, a floe will have an individual response, in which the floe itself flexes and scatters the wave in the surrounding free surface. Notwithstanding this, when a number of floes is present, we must also take account of the interaction of the floes by considering the simultaneous dependence of each floe on the waves scattered by the other floes. So, in addition to the individual response of the floes, for multiple floes there is a net response of the conglomeration to consider as well.

Due to the complexity of the coupling between the ice and fluid, it is often assumed that floes are of a uniform thickness and have zero draught in order to facilitate a solution. However, by using a variational principle and associating the vertical motion with the mode that supports propagating waves, Porter and Porter (2004) were able to correctly derive approximations for 2-dimensional floes of varying thickness and Archimedian draught. This approximation was later extended to a full-linear solution by Bennetts, Biggs and Porter (2007) by including a finite number of the modes that support evanescent waves.

A number of papers has investigated the way in which 3-dimensional ice floes react to and scatter incident waves. It is usual to assume some simplification of the shape of the floe in order that a solution may be found. For instance, Meylan and Squire (1995), Peter, Meylan and Wang (2004) and Andrianov and Hermans (2004) all treat the case of a circular floe of uniform thickness and a zero draught. Other papers have attempted to elaborate on this structure. Meylan (2002), for example, constructs a method based on the numerical evaluation of the in vacuo modes of the plate to generate solutions for a floe of uniform thickness and a zero draught, but where the shape of the floe is arbitrary. Using the multi-mode expansion of the vertical motion noted above, Bennetts, Biggs and Porter (2008) investigated the case of a circular floe of a non-zero draught and axisymmetrically varying thickness.

It is widely recognised, however, that in order to assess the scattering of waves in the MIZ we must consider a model that comprises a large number of individual floes, in which floes interact with one another as well as with the incident wave. To this end, some research has been conducted on multiple floe arrays. Peter and Meylan (2004) extended Meylan (2002) through the use of local coordinate systems and Graf's addition theorem in order to combine the effects of a finite number of individual floes. In this case, the computational sustainability of the method becomes strained as the number of constituent floes increases. For this reason, unphysical periodic problems, involving an infinite number of arrays, have been studied in order to represent a large number of floes whilst keeping the numerics manageable. In one such paper, Peter, Meylan and Linton (2006) build upon the work of Peter and Meylan (2004) and invoke periodicity to solve for a straight-line array of identical ice floes on a fluid domain that stretches to infinity in all lateral directions. Wang, Meylan and Porter (2007) consider the same problem as Peter, Meylan and Linton (2006) but use a periodic Green's function as their method of solution.

In the work outlined in this paper, we also consider a straight-line array of equispaced, identical floes on an infinite fluid surface. However, unlike Peter, Meylan and Linton (2006) and Wang, Meylan and Porter (2007), we allow our floes to vary in thickness

Received January 24, 2008; revised manuscript received by the editors July 31, 2008. The original version (prior to the final revised manuscript) was presented at the 18th International Offshore and Polar Engineering Conference (ISOPE-2008), Vancouver, July 6–11, 2008.
KEY WORDS: Array, Green's function, sea ice, scattering, periodic.

and possess a non-zero draught, and we apply an assumption of axisymmetry to the floes. It is shown that the problem may be considered in a single channel that extends to infinity in one horizontal direction and finitely in the other, and contains a single floe. The variational principle and single-mode approximation of Porter and Porter (2004) are then invoked to generate a set of governing equations in the horizontal plane only, and these are solved by the use of a Green's function in the free-surface region and a Fourier expansion of the unknowns in the ice-covered region. This leaves a set of ordinary differential equations (ODE) to be solved numerically over the radius of the floe.

The motivation for studying this problem is that we can better represent situations in the MIZ at a low numerical cost. In conclusions, a proposition is made for the natural extension of the method outlined in our work to multiple arrays of periodic straight-line floes. Further, the possibility exists of adding semi-infinite regions of continuous ice cover to one or both sides of the multiple arrays. Such a model could then be thought of as representing the interface of the MIZ with the open ocean, or pancake ice that forms in the leads that occupy the MIZ.

FORMULATION OF PROBLEM

We wish to solve the problem of a straight-line array of identical axisymmetric floes, which are permitted to vary in thickness (through both their upper and lower surfaces) and have a non-zero draught. The Cartesian coordinates x and y will be used to denote horizontal position, with z being the vertical coordinate. The plane $z=0$ is set to coincide with the equilibrium fluid surface, and the bed (considered flat and finite) lies at $z=-h$. Without loss of generality, we orient our horizontal coordinates so that the centre of the floes occupies the y-axis, with one floe having its centre at the origin $(x,y)=(0,0)$. Hence, if we let the distance between the centre of adjacent floes be $2y_0$, for some positive constant y_0, then the centres of the floes are the points $y=2ny_0$ $(n\in\mathbb{N})$.

Assuming the regular properties of linear motion, the motion of the fluid may be defined through a reduced velocity potential, $\Phi=\Phi(x,y,z)$, which, for time-harmonic conditions, is such that the velocity field is retrieved from $\Re\mathrm{e}\{(g/i\omega)(\partial_x,\partial_y,\partial_z)\cdot(\Phi\,\mathrm{e}^{-\mathrm{i}\omega t})\}$. Here, $g=9.81\,\mathrm{m\,s^{-2}}$ denotes gravitational acceleration, and ω is a prescribed angular frequency. When forced by a wave, the underside of each floe experiences small-amplitude oscillations. The position of the fluid-ice interface is then defined to be:

$$z=-d(x,y)+\Re\mathrm{e}\{W(x,y)\,\mathrm{e}^{-\mathrm{i}\omega t}\},$$

for (x,y) within the ice-covered regions. The surface $z=-d$ denotes the equilibrium position of the lower surface of the floes, with $d=0$ outside the ice-covered region. The function W is the reduced displacement of the floes, and for consistency we may set W to define the free surface outside the ice-covered regions (although this will not be used in practice). We are now required to solve for the velocity potential, Φ, in the fluid domain and the displacement, W, within the ice-covered regions.

When the array is forced by a plane incident wave, a periodicity condition is induced:

$$\Phi(x,y+2y_0,z)=\mathrm{e}^{2\mathrm{i}uy_0}\,\Phi(x,y,z), \tag{1a}$$

and:

$$\partial_y\Phi(x,y+2y_0,z)=\mathrm{e}^{2\mathrm{i}uy_0}\,\partial_y\Phi(x,y,z), \tag{1b}$$

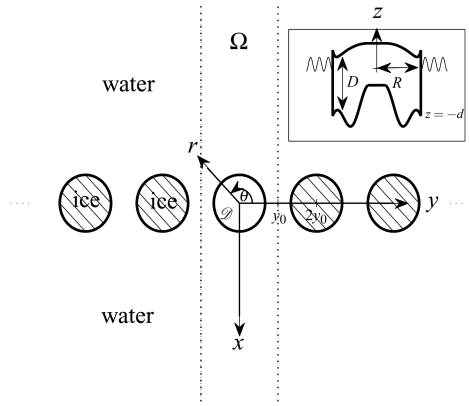

Fig. 1 Plan view of geometrical configuration with cross-section of axisymmetric floe shown in inset

with similar expressions holding for the displacement function W. The quantity u is related to the forcing wave and is considered known during the formulation of the scattering problem.

It is then possible to solve for the infinite array by considering a single channel of width $2y_0$ in the y-direction. For simplicity, we will take this channel to be $(x,y)\in\Omega=\{x,y:-\infty<x<\infty,-y_0<y<y_0\}$ and $z\in(-h,-d)$. At this point we define the single floe contained within this channel to occupy the region $(r,\theta)\in\mathscr{D}=\{r,\theta:r<R,0<\theta<2\pi\}$, where R denotes the radius of the floe. Due to the circular shape of the floe, the polar coordinates $r=\sqrt{x^2+y^2}$ and $\theta=\tan^{-1}(y/x)$ will be used for convenience in place of x and y in $\mathscr{D}$. Under the imposed axisymmetric conditions in $\mathscr{D}$ we have $d=d(r)$, and also $D=D(r)$, where D denotes the thickness of the ice. Further, we will define $H(r)=h-d(r)$ to be the fluid depth beneath the floe.

Within the fluid domain the velocity potential must satisfy Laplace's equation:

$$\nabla^2\Phi+\partial_z^2\Phi=0,\quad((x,y)\in\Omega,z\in(-h,-d)),$$

where $\nabla=(\partial_x,\partial_y)$ or $\nabla=(\cos(\theta)\partial_r-(1/r)\sin(\theta)\partial_\theta,\sin(\theta)\partial_r+(1/r)\cos(\theta)\partial_\theta)$ depending on the context, and on the bed $(z=-h)$ the no-flow condition $\partial_z\Phi=0$ for $(x,y)\in\Omega$ holds. At the fluid-ice interface $(z=-d)$ we have high-order conditions that define the dynamics of the floe's oscillations and in doing so couple the velocity potential to the displacement function. These conditions are given as:

$$(1-\sigma\alpha)W+\mathscr{L}W-\Phi=0\quad((x,y)\in\mathscr{D},\,z=-d), \tag{2a}$$

and:

$$\nabla d\cdot\nabla\Phi+\partial_z\Phi=0\quad((x,y)\in\mathscr{D},\,z=-d), \tag{2b}$$

where $\mathscr{L}=\nabla^2\beta\nabla^2+(1/r)(1-\nu)\{\partial_r(\partial_r\beta)\partial_r+(1/r)(\partial_r^2\beta)\partial_\theta^2\}$. The various quantities are defined as $\nu=0.3$, which is Poisson's ratio; $\sigma=\omega^2/g$, the frequency parameter; $\alpha=\alpha(r)=\rho_iD/\rho_w$, the scaled mass of the floe; and $\beta=\beta(r)=ED^3/12(1+\nu)\rho_wg$, the scaled flexural rigidity of the floe. Further parameters have been introduced in these definitions: the mass of the ice $\rho_i=922.5\,\mathrm{kg\,m^{-3}}$; the mass of the fluid $\rho_w=1025\,\mathrm{kg\,m^{-3}}$; and Young's modulus $E=5\times10^9\,\mathrm{Pa}$. At the ice edge, $r=R$, 2 further dynamic conditions must hold; they state that the bending moment and shearing stress must vanish. These conditions are expressed as $\mathscr{B}W=0$ and $\mathscr{S}W=0$, respectively, where:

$$\mathscr{B}=\beta\nabla^2-\frac{1}{r}(1-\nu)\beta\left\{\partial_r+\frac{1}{r}\partial_\theta^2\right\} \tag{3a}$$

and:

$$\mathscr{S} = \partial_r(\beta\nabla^2) + \frac{1}{r}(1-\nu)\left\{(\partial_r\beta)\left(\partial_r - \frac{1}{r}\partial_\theta^2\right) - \beta\partial_r\left(\frac{1}{r}\partial_\theta^2\right)\right\}. \quad (3b)$$

We translate the periodicity of the solution given in Eqs. 1a and b into transition conditions on the sides of the channel to give:

$$\Phi(x, y_0, z) = \mathrm{e}^{2\mathrm{i}uy_0}\,\Phi(x, -y_0, z), \quad (4a)$$

and:

$$\partial_y\Phi(x, y_0, z) = \mathrm{e}^{2\mathrm{i}uy_0}\,\partial_y\Phi(x, -y_0, z). \quad (4b)$$

The problem is fully defined by imposing the far-field radiation conditions:

$$\Phi(x,y,z) \sim \left\{\mathrm{e}^{\mathrm{i}(v_0x+u_0y)} + \sum_{m\in M} R_m\mathrm{e}^{\mathrm{i}(-v_mx+u_my)}\right\}\cosh\{k(z+h)\} \quad (5a)$$

as $x\to-\infty$, and:

$$\Phi(x,y,z) \sim \left\{\sum_{m\in M} T_m\mathrm{e}^{\mathrm{i}(v_mx+u_my)}\right\}\cosh\{k(z+h)\} \quad (5b)$$

as $x\to\infty$, where $u_m = u + m\pi/y_0$ and $v_m = \sqrt{k^2-u_m^2}$ ($m\in\mathbb{N}$), and M is the subset of natural numbers for which the v_m are real. The quantity k is the propagating wavenumber that will be defined shortly. These radiation conditions express a single incident wave $\phi^I(x,y)\cosh\{k(z+h)\} = \mathrm{e}^{\mathrm{i}(v_0x+u_0y)}\cosh\{k(z+h)\}$, which propagates from $x\to-\infty$ and is partially reflected and partially transmitted in the form of a finite number of waves with known angles. All remaining motions generated in the scattering process have evanesced by the time they reach the far-field.

Approximation

Due to the complexity of the problem in hand we will seek an approximation method. We choose to write:

$$\Phi(x,y,z) \approx \begin{cases}\phi(x,y)\cosh\{k(z+h)\} & (x,y)\in\Omega/\mathscr{D},\\ \psi(r,\theta)\cosh\{\kappa(z+h)\} & (x,y)\in\mathscr{D}.\end{cases} \quad (6)$$

Here k is the propagating wavenumber in the free-surface region, defined as the real root of the free-surface dispersion relation:

$$k\tanh(kh) = \sigma, \quad (7a)$$

and $\kappa = \kappa(r)$ is the analogous propagating wavenumber in the ice-covered region, which is the real root of the ice-covered dispersion relation:

$$(1-\sigma\alpha+\beta k^4)k\tanh(kH) = \sigma. \quad (7b)$$

The motivation behind the form of Eq. 6 is based on a mild-slope approximation, in which we assume that the geometrical variations are small in comparison with the wavelengths of the problem.

When applied in the variational principle given in Porter and Porter (2004), which is equivalent to the governing equations presented above, a new set of governing equations is generated. From these new equations we must calculate the unknown functions ϕ and ψ, along with an approximation of the displacement function $W(x,y)\approx\chi(r,\theta)$ that is produced indirectly. In the free-surface region, it remains to solve the Helmholz equation:

$$\nabla^2\phi + k^2\phi = 0 \quad ((x,y)\in\Omega/\mathscr{D}). \quad (8)$$

For the ice-covered disc, we now have a 2nd-order equation coupled to a 4th-order equation:

$$\nabla(a\nabla\psi) + b\psi + \sigma\cosh(\kappa H)\chi = 0 \quad (r,\theta)\in\mathscr{D}, \quad (9a)$$

and:

$$(1-\sigma\alpha)\chi + \mathscr{L}\chi - \cosh(\kappa H)\psi = 0 \quad (r,\theta)\in\mathscr{D}, \quad (9b)$$

where the values of the coefficients $a = a(r)$ and $b = b(r)$ are functions of the radial coordinate only. Their values may be calculated from the expressions:

$$a = \int_{-h}^{-d}\cosh^2\{\kappa(z+h)\}\mathrm{d}z \quad (10a)$$

and:

$$b = \sigma^2 a - \kappa\sinh(2\kappa H)/2 - \int_{-h}^{-d}\left\{(\partial_r\cosh\{\kappa(z+h)\})^2\right\}\mathrm{d}z + \partial_r\int_{-h}^{-d}\{\cosh\{\kappa(z+h)\}(\partial_r\cosh\{\kappa(z+h)\})\}\,\mathrm{d}z. \quad (10b)$$

Note that, through use of a variational principle in conjunction with Eq. 6, we have created a process of vertical averaging, and in doing so have eliminated the coordinate z from our new set of governing equations.

In Eq. 6 there is a partitioning of the solution between the ice-covered and free-surface regions. This has the effect of creating a discontinuity in the velocity potential at the edge of the floe ($r = R$), and the functions ϕ and ψ must thus be linked through jump conditions at this interface. These jump conditions are provided by the variational principle, and we choose to write them in the form:

$$\phi = j_0\psi, \quad \partial_r\phi = j_1\partial_r\psi + j_2\psi, \quad (11)$$

for known constants j_i ($i = 0, 1, 2$). The occurrence of such jumps in the approximation somewhat contradicts the supposition of mild-slopes. Studies of the accuracy of the single-mode approximation are made in Bennetts (2007) and Bennetts, Biggs and Porter (2007) for more simple geometries. From their findings we expect our approximation to give generally excellent results but that it will become compromised by floes with thick edges and for high-frequency waves. Further, it is possible to extend our single-mode approximation to a multi-mode approximation by using the approach of Bennetts, Biggs and Porter (2007). In fact, the solution method that we describe below is readily applied to the multi-mode approximation, and this work is currently in preparation.

The transition boundary conditions for Φ, given in Eqs. 4a and b, are similarly satisfied by ϕ, so that:

$$\phi(x,y_0) = \mathrm{e}^{2\mathrm{i}uy_0}\,\Phi(x,-y_0),$$
$$\partial_y\phi(x,y_0) = \mathrm{e}^{2\mathrm{i}uy_0}\,\partial_y\phi(x,-y_0). \quad (12)$$

Similarly, the radiation conditions (Eq. 5) are easily retained in the approximation:

$$\phi(x,y) \sim \begin{cases} \left\{ \mathrm{e}^{\mathrm{i}(\nu_0 x + u_0 y)} + \sum_{m\in M} R_m \, \mathrm{e}^{\mathrm{i}(-\nu_m x + u_m y)} \right\} & (x \to -\infty), \\ \sum_{m\in M} T_m \, \mathrm{e}^{\mathrm{i}(\nu_m x + u_m y)} & (x \to \infty). \end{cases} \tag{13}$$

Notice that this is a consequence of our choice of vertical mode in the free-surface region, and it is an important feature of the approximation.

As it is indirectly approximated, the conditions applied to the displacement function remain as $\mathscr{B}\chi = \mathscr{S}\chi = 0$ on the ice edge $\mathscr{C}$.

Solution Process

As it now stands, we may consider our task in terms of 2 disjoint problems. In the first, we consider the solution ϕ of the free-surface problem posed by the Helmholz Eq. 8 in $\Omega/\mathscr{D}$, subject to the transition conditions (Eqs. 12a and b) and radiation conditions (Eq. 13). Scattering is caused by the relation to the as-yet unknown function ψ and its radial derivative on the boundary $\mathscr{C} = \{x, y : x^2 + y^2 = R\}$. For the second problem, we must obtain ψ and χ as the solutions to the 6th-order system of differential equations (Eqs. 9a and b) in the disc $\mathscr{D}$, where χ satisfies the bending moment and shearing stress conditions at the edge $\mathscr{C}$. Forcing is provided through ψ from the jump conditions (Eq. 11) at $\mathscr{C}$. Once the solutions have been obtained in their respective regions, up to unknown factors, we will complete the solution through the imposition of these jump conditions. As the 2 domains Ω and $\mathscr{D}$ are fundamentally different, one being structured on Cartesian coordinates and the other on polar coordinates, we are unable to obtain a solution through use of any direct modal expansion. Instead, we will pursue a method in which we treat each domain independently, and finally match the derived representations at the common boundary ($r = R$).

Free-Surface Domain

Consider first the free-surface domain $\Omega/\mathscr{D}$. Let the Green's function $G = G(x, y|\xi, \eta)$ be defined over the entire channel Ω in the absence of the floe, so that it satisfies the equations:

$$\nabla^2 G + k^2 G = \delta(x-\xi)\delta(y-\eta) \quad ((x,y) \in \Omega).$$

On the lateral boundaries $y = \pm y_0$, we impose the transition conditions:

$$G(x, y_0) = \mathrm{e}^{-2\mathrm{i}uy_0} \, G(x, -y_0),$$
$$\partial_y G(x, y_0) = \mathrm{e}^{-2\mathrm{i}uy_0} \, \partial_y G(x, -y_0),$$

which are the reciprocal conditions to those satisfied by ϕ. Finally, we require that G represent outgoing waves in the far-fields $x \to \pm\infty$. The Green's function G is easily found via expansion in the modes $\mathrm{e}^{-\mathrm{i}u_m(y-\eta)}$ ($m \in \mathbb{N}$) to be:

$$G(x, y|\xi, \eta) = \frac{1}{4\mathrm{i}y_0} \sum_{m=-\infty}^{\infty} \frac{\mathrm{e}^{\mathrm{i}\nu_m|x-\xi|} \, \mathrm{e}^{-\mathrm{i}u_m(y-\eta)}}{\nu_m}. \tag{14}$$

This form of G has been calculated and utilised previously; see, for instance, Porter and Porter (2003).

Applying Green's second identity to ϕ and G over the domain $\Omega/\mathscr{D}$, we deduce the representations:

$$\phi(\xi,\eta) = \phi^I(\xi,\eta) - R\int_0^{2\pi} \{\phi\partial_r G - G\partial_r\phi\}_{r=R} \, \mathrm{d}\theta, \tag{15a}$$

for $(\xi, \eta) \in \Omega/\mathscr{D}$, and:

$$\frac{1}{2}\phi(\xi,\eta) = \phi^I(\xi,\eta) - R\int_0^{2\pi} \{\phi\partial_r G - G\partial_r\phi\}_{r=R} \, \mathrm{d}\theta, \tag{15b}$$

for $(\xi, \eta) \in \mathscr{C}$.

Ice-covered Domain

Next, we consider the ice-covered domain $\mathscr{D}$. The method we utilise here is a modification of that of Bennetts, Biggs and Porter (2008), who considered a solitary axisymmetric ice floe.

Let the unknowns be written in terms of the Fourier expansions:

$$\psi(r,\theta) = \sum_{n=-N}^{N} \psi_n(r) \, \mathrm{e}^{\mathrm{i}n\theta}, \quad \chi(r,\theta) = \sum_{n=-N}^{N} \chi_n(r) \, \mathrm{e}^{\mathrm{i}n\theta}, \tag{16}$$

which, for the purposes of numerical calculation, we have truncated to a finite dimension that will give sufficient accuracy. Due to the assumed axisymmetry of the geometry, the governing equations (Eqs. 9a and b) decouple into a set of ODE in the radial coordinate, which may be solved independently for each Fourier mode. We choose to write these decoupled equations as the 2nd-order systems:

$$\frac{1}{r}(rA\mathbf{u}_n')' + B_n\mathbf{u}_n = \mathbf{0} \quad (n = -N, \ldots, N), \tag{17}$$

for $0 < r < R$, where a prime denotes differentiation with respect to r, and the vectors of unknowns are $\mathbf{u}_n = \mathbf{u}_n(r) = (\psi_n(r), \chi_n(r), \hat{\chi}_n(r))^T$, with $\hat{\chi}_n \equiv \beta(\chi_n'' + \chi_n'/r - n^2\chi_n/r^2)$. The matrices $A = A(r)$ and $B_n = B_n(r)$ are defined as:

$$A = \begin{pmatrix} a & 0 & 0 \\ 0 & 1 & 0 \\ 0 & -(1-\nu)\dfrac{1}{r}\beta & 1 \end{pmatrix}, \tag{18}$$

and:

$$B_n = \begin{pmatrix} b - \dfrac{n^2}{r^2}a & \sigma\cosh(\kappa H) & 0 \\ 0 & 0 & -1/\beta \\ -\cosh(\kappa H) & (1-\nu)\dfrac{n^2}{r^2}\beta'' + 1 - \sigma\alpha & -\dfrac{n^2}{r^2} \end{pmatrix}, \tag{19}$$

where a and b are defined in Eqs. 10a and b.

The boundary data required for the above ODE are provided by the jump conditions $j_0\psi_n(R) = \phi_n(R)$ and $j_1\psi_n'(R) + j_2\psi_n(R) = \phi_n'(R)$, and the dynamic conditions:

$$\mathscr{B}_n(\hat{\chi}_n, \chi_n) \equiv \hat{\chi}_n - (1-\nu)\beta\left(\frac{1}{r}\chi_n' - \frac{n^2}{r^2}\chi_n\right) = 0, \tag{20a}$$

and:

$$\mathscr{S}_n(\hat{\chi}_n, \chi_n) \equiv \hat{\chi}_n' - (1-\nu)\left\{\beta'\left(\frac{1}{r}\chi_n' - \frac{n^2}{r^2}\chi_n\right) + n^2\beta\frac{1}{r}\left(\frac{1}{r}\chi'\right)\right\} = 0, \tag{20b}$$

at $r = R$. These are derived by applying the Fourier expansions (Eq. 16), along with the equivalent expansion $\phi(x,y) \approx \sum_{n=-N}^{N} \phi_n(r) \, \mathrm{e}^{in\theta}$ of the free-surface potential, to the analogous expressions (Eq. 11) and (Eqs. 3a and b). As the jump conditions

involve the as-yet unknown value of the free-surface potential ϕ and its radial derivative on the edge of the floe ($r = R$), it is not possible to calculate the functions $\mathbf{u}_n$ explicitly. Instead, we express each of the vectors $\mathbf{u}_n$ in terms of the as-yet unknown factor $\phi'_n(R)$, and this may be achieved by writing:

$$\mathbf{u}_n(r) = \phi'_n(R)\mathbf{v}_n(r), \tag{21}$$

where $\mathbf{v}_n = (v_{n,0}, v_{n,1}, v_{n,2})^T$ satisfies the appropriate ODE of Eq. 17 and the conditions:

$$j_1 v'_{n,0} + j_2 v_{n,0} = 1,$$

and:

$$\mathscr{B}_n(v_{n,2}, v_{n,1}) = \mathscr{S}_n(v_{n,2}, v_{n,1}) = 0,$$

at $r = R$.

At the centre of the floe we require that the solution be bounded. However, the use of the radial coordinates introduces a singularity at this point. In order to deal with this efficiently in our numerical solution, we mimic Bennetts, Biggs and Porter (2008) by assuming the existence of a disc of arbitrarily small radius ϵ around the centre of the floe, within which the geometry of the ice is uniform.

We are then able to eliminate the singularity analytically, and this leads to the condition $J_{n,1}\mathbf{v}'_n + J_{n,2}\mathbf{v}_n = \mathbf{0}$ ($n = -N, \ldots, N$) at $r = \epsilon$, where $J_{n,1}$ and $J_{n,2}$ are known matrices. In practice we then simply let the value of ϵ tend to zero until we achieve convergence.

The vectors $\mathbf{v}_n$ are then calulated for $n = -N, \ldots, N$, by solving the ODE of Eq. 17 numerically over the interval $r \in (\epsilon, R)$ and imposing the given boundary conditions. Note that $B_n = B_{-n}$ and the boundary conditions are identical for n, and $-n$ implies that $\mathbf{v}_n = \mathbf{v}_{-n}$, and we thus need only calculate the solutions within the disc, $\mathbf{v}_n$, for $n = 0, \ldots, N$.

Matching at Ice Edge

We now have at our disposal expressions for each Fourier mode of the solution within the ice-covered domain, but they contain the as-yet unknown quantities $\phi'_n(R)$ ($n = -N, \ldots, N$), while in the free-surface region we have the integral forms (Eqs. 15a and b) for the approximate velocity potential. It is necessary to match these representations at their common boundary, the ice edge $r = R$, in order to calculate the solution throughout the channel Ω.

Amalgamating our representation for the Fourier modes of the velocity potential ψ at the ice edge into one expression, and using the jump conditions $\phi_n = j_0\psi_n$, we have:

$$j_0\mathbf{f}_0 = M\mathbf{f}_1. \tag{22}$$

Here, the vectors $\mathbf{f}_0$ and $\mathbf{f}_1$ are defined as:

$$\mathbf{f}_0 = (\phi_{-N}(R), \ldots, \phi_N(R))^T,$$

and:

$$\mathbf{f}_1 = (\phi'_{-N}(R), \ldots, \phi'_N(R))^T.$$

In Eq. 22, M is the diagonal matrix:

$$M = \mathrm{diag}(v_{-N,0}(R), \ldots, v_{N,0}(R)).$$

We have thus so far produced a system of $2N + 1$ equations in the $4M + 2$ unknowns contained in $\mathbf{f}_0$ and $\mathbf{f}_1$.

The remaining $2N + 1$ equations required to solve for the p_i ($i = 0, 1$) are provided by our integral representation of ϕ on the ice edge given in Eq. 15b. If we use our Fourier expansion of ϕ here, namely $\phi(x, y) = \sum_{n=-N}^{N} \phi_n(r)\,\mathrm{e}^{\mathrm{i}n\theta}$, and take the $2N + 1$ inner-products with respect to $\mathrm{e}^{-\mathrm{i}m\tau}$ ($m = -N, \ldots, N$) over $\tau \in (0, 2\pi)$, then we may interpret Eq. 15b as the matrix system:

$$\frac{1}{2}\mathbf{f}_0 = \mathbf{f}_I - R\big(\widetilde{Q}\mathbf{f}_0 - Q\mathbf{f}_1\big). \tag{23}$$

In Eq. 23, the vector $\mathbf{f}_I$ contains the inner products of the incident wave, which are:

$$\{\mathbf{f}_I\}_{N+1+n} = \frac{1}{2\pi}\int_0^{2\pi} [\phi^I\,\mathrm{e}^{-\mathrm{i}n\tau}]_{r=R}\,\mathrm{d}\tau,$$

for $n = -N, \ldots, N$. By using Graf's addition formulae for Bessel functions (Abramowitz and Stegun, 1964) to rewrite the incident wave in terms of the polar coordinates, we may calculate this integral explicitly to be:

$$\{\mathbf{f}_I\}_{N+1+n} = \mathrm{e}^{\mathrm{i}n\vartheta}\,\mathrm{J}_n(kR) \quad (n = -N, \ldots, N),$$

where ϑ is the angle such that $\tan\vartheta = v_0/u_0$ existing in the interval $0 < \vartheta < \pi/2$.

The matrices in Eq. 23 are:

$$\{Q\}_{N+1+n,N+1+m} = \frac{1}{2\pi}\int_0^{2\pi}\int_0^{2\pi} [G\,\mathrm{e}^{\mathrm{i}(n\theta - m\tau)}]\,\mathrm{d}\theta\,\mathrm{d}\tau, \tag{24a}$$

and:

$$\{\widetilde{Q}\}_{N+1+n,N+1+m} = \frac{1}{2\pi}\int_0^{2\pi}\int_0^{2\pi} [(\partial_r G)\,\mathrm{e}^{\mathrm{i}(n\theta - m\tau)}]\,\mathrm{d}\theta\,\mathrm{d}\tau, \tag{24b}$$

for $n, m = -N, \ldots, N$. By using Graf's addition theorem for Bessel functions, it is possible to calculate explicit expressions for these matrix entries in a fashion similar to that we used for the entries of the vector $\mathbf{f}_I$. However, it turns out that these expressions are numerically impractical, and we instead employ numerical techniques to evaluate the integrals appearing in Eqs. 24a and b. In order to proceed in this manner, we must note that Green's function G contains a logarithmic singularity at the point $(x, y) = (\xi, \eta)$, and in order to avoid using many of the terms of the infinite expansion of G given in Eq. 14, we must work to extricate this singularity.

We begin by denoting the series representation of Green's function (Eq. 14) as $G = \sum_{m=-\infty}^{\infty} s_m$ where:

$$s_m = \frac{1}{4\mathrm{i}y_0 v_m}\,\mathrm{e}^{\mathrm{i}v_m|x-\xi| - \mathrm{i}u_m(y-\eta)}.$$

The logarithmic singularity is manifest as a divergence of this series at the point of intersection of the field and source variables, where we have $s_n \sim 1/n$ for large n. If we let the terms:

$$t_{m,\pm} = \frac{-1}{4m\pi}\,\mathrm{e}^{-(u + m\pi/y_0)|x-\xi| - \mathrm{i}(u \pm m\pi/y_0)(y-\eta)}$$

for $m = 1, \ldots,$ then it is a simple matter to show that the series $\sum_{m=1}^{\infty}\{s_m - t_{m,+}\}$ and $\sum_{m=1}^{\infty}\{s_{-m} - t_{m,-}\}$ both converge at all

points, including $(x, y) = (\xi, \eta)$, which is to the order $1/n^3$. So, by rewriting the Green's function as:

$$G = s_0 + \sum_{m=1}^{\infty} \{s_{\pm m} - t_{m,\pm}\} + \sum_{m=1}^{\infty} t_{m,\pm}$$
$$= s_0 + \sum_{m=1}^{\infty} \{s_{\pm m} - t_{m,\pm}\} + \frac{1}{4\pi} p_0 \ln(p),$$

where:

$$p_0 = \mathrm{e}^{Ru\{|\cos(\theta)-\cos(\tau)|-\mathrm{i}(\sin(\theta)-\sin(\tau))\}}$$

and:

$$p = 1 - 2\mathrm{e}^{-R\pi|\cos(\theta)-\cos(\tau)|/y_0} \cos\big(\pi(\sin(\theta)-\sin(\tau))/y_0\big) + \mathrm{e}^{-2R\pi|\cos(\theta)-\cos(\tau)|/y_0},$$

it is given by the sum of a rapidly convergent series and a logarithmic function. Thus, we have transfered the singularity into the log term, so that it is now explicit. Our aim is to use this expression in Eq. 24a and perform the integration of the singularity analytically. To achieve the latter, first consider the integral:

$$\int_0^{2\pi}\int_0^{2\pi} p_0 \ln(p)\, \mathrm{e}^{\mathrm{i}(n\theta - m\tau)}\, \mathrm{d}\theta\, \mathrm{d}\tau,$$

which will be more convenient to write as:

$$\int_0^{2\pi}\int_0^{2\pi} p_0 \ln\left(\frac{p}{q}\right) \mathrm{e}^{\mathrm{i}(n\theta - m\tau)}\, \mathrm{d}\theta\, \mathrm{d}\tau + \int_0^{2\pi}\int_0^{2\pi} \ln(q)\big(p_0\, \mathrm{e}^{\mathrm{i}(n\theta - m\tau)} - \mathrm{e}^{\mathrm{i}(n-m)\tau}\big)\mathrm{d}\theta\, \mathrm{d}\tau + \int_0^{2\pi}\int_0^{2\pi} \ln(q)\, \mathrm{e}^{\mathrm{i}(n-m)\tau}\, \mathrm{d}\theta\, \mathrm{d}\tau,$$

where $q = 2(R\pi/y_0)^2(1-\cos(\theta-\tau))$. The functions appearing in the initial 2 integrals do not contain singularities, which has been moved into the more appealing function that requires integration in the final term. We may calculate this analytically to be:

$$\int_0^{2\pi}\int_0^{2\pi} \ln(q)\, \mathrm{e}^{\mathrm{i}(n-m)\tau}\, \mathrm{d}\theta\, \mathrm{d}\tau = \begin{cases} 8\pi^2 \ln(R\pi/y_0) & (m = n), \\ 0 & (m \neq n). \end{cases}$$

The integral entries of the matrix Q are now all easily numerically calculable.

Similarly, let the radial derivative of the Green's function be denoted as: $\partial_r G = \sum_{m=-\infty}^{\infty} \widetilde{s}_m$ where:

$$\tilde{s}_m = \begin{cases} \dfrac{v_m \cos(\theta) - u_m \sin(\theta)}{4 y_0 v_m}\, \mathrm{e}^{\mathrm{i}v_m(x-\xi) - \mathrm{i}u_m(y-\eta)} & (\cos(\theta) > \cos(\tau)), \\ \dfrac{-v_m \cos(\theta) - u_m \sin(\theta)}{4 y_0 v_m}\, \mathrm{e}^{-\mathrm{i}v_m(x-\xi) - \mathrm{i}u_m(y-\eta)} & (\cos(\theta) > \cos(\tau)). \end{cases} \quad (25)$$

Defining the terms:

$$\tilde{t}_{m,\pm} = \begin{cases} \dfrac{\mathrm{e}^{\mp \mathrm{i}\theta}}{4y_0}\, \mathrm{e}^{-(u_0 + m\pi/y_0)(x-\xi) - \mathrm{i}(u_0 \pm m\pi/y_0)(y-\eta)} & (\cos(\theta) > \cos(\tau)), \\ \dfrac{-\mathrm{e}^{\pm \mathrm{i}\theta}}{4y_0}\, \mathrm{e}^{(u_0 + m\pi/y_0)(x-\xi) - \mathrm{i}(u_0 \pm m\pi/y_0)(y-\eta)} & (\cos(\theta) > \cos(\tau)), \end{cases}$$

for $m = 1, \ldots,$ and by summing infinite series involving these terms, we are able to rewrite $\partial_r G$ in the form:

$$\partial_r G = \widetilde{s}_0 + \sum_{m=1}^{\infty} \{\widetilde{s}_{\pm m} - \widetilde{t}_{m,\pm}\} + \frac{p_0 p_1 p_2}{2 y_0 p}, \quad (26)$$

where:

$$p_1 = \begin{cases} \cos(R\pi(\sin(\theta) - \sin(\tau))/y_0 - \theta) \\ \qquad - \cos(\theta) p_2(\theta, \tau) & (\cos(\theta) > \cos(\tau)), \\ \cos(R\pi(\sin(\theta) - \sin(\tau))/y_0 + \theta) \\ \qquad - \cos(\theta) p_2(\theta, \tau) & (\cos(\theta) > \cos(\tau)), \end{cases}$$

and:

$$p_2 = \begin{cases} \mathrm{e}^{-R\pi(\cos(\theta) - \cos(\tau))} & (\cos(\theta) > \cos(\tau)), \\ \mathrm{e}^{R\pi(\cos(\theta) - \cos(\tau))} & (\cos(\theta) > \cos(\tau)). \end{cases}$$

This again gives us a representation involving a series that converges far faster than that appearing in the original expression (Eq. 25), along with a potentially singular term in closed form. By using l'Hôpital's rule twice, it is possible to show that, at the point $(x, y) = (\xi, \eta)$, the fraction $p_0 p_1 / p$ is in fact bounded and we have:

$$\lim_{\theta \to \tau} \left(\frac{p_0 p_1}{p}\right) = \begin{cases} 1 - R\pi \cos(\tau)/y_0 & (x > \xi), \\ -(1 + R\pi \cos(\tau)/y_0) & (x < \xi). \end{cases}$$

There is then no more that we need to do to Eq. 26 to allow ourselves to evaluate the integrals appearing in the matrix $\widetilde{Q}$ numerically.

Finally, in our evaluation of the matrices Q and $\widetilde{Q}$, we note the symmetries:

$$Q_{N+1+n,N+1+m} = Q_{N+1+m,N+1+n},$$

$$Q_{N+1+n,N+1+m} = (-1)^{n+m} Q_{N+1-n,N+1-m},$$

and:

$$\widetilde{Q}_{N+1+n,N+1+m} = (-1)^{n+m} \widetilde{Q}_{N+1-n,N+1-m},$$

for $n, m = -N, \ldots, N$. The use of these symmetries constitutes a considerable numerical saving.

Note that, unlike Eq. 22, the matrix system (Eq. 23) is not diagonal and thus couples the Fourier modes. Having calculated the entries of the vector of integrals of the incident wave, $\mathbf{f}_I$, and the matrices of integrals of the Green's function and its radial derivative, Q and $\widetilde{Q}$, it is now possible to solve for the vectors of unknowns $\mathbf{f}_0$ and $\mathbf{f}_1$. To do this we use Eq. 23 to express $\mathbf{f}_1$ in terms of $\mathbf{f}_I$ and $\mathbf{f}_0$, with:

$$\mathbf{f}_1 = \frac{1}{R} Q^{-1} \mathbf{f}_I - Q^{-1}\left(\frac{1}{2R} I + \widetilde{Q}\right)\mathbf{f}_0. \quad (27)$$

Using Eq. 27 to eliminate $\mathbf{f}_1$ from Eq. 22 leaves the system of $2N + 1$ equations:

$$\left(I + \frac{1}{2R} M Q^{-1} + M\widetilde{Q}\right)\mathbf{f}_0 = \frac{1}{R} M Q^{-1} \mathbf{f}_I, \quad (28)$$

in the $2N+1$ unknowns contained in the vector $\mathbf{f}_0$, with the known forcing vector $\mathbf{f}_I$.

Using Eq. 28, we may calculate the vector $\mathbf{f}_0$ through inversion of the $(2N+1)$-dimensional matrix on the left-hand side. We then obtain $\mathbf{f}_1$ directly via Eq. 27, which provides us with the information needed to fully define the solution in the ice-covered region using expressions given in Eq. 21.

Having obtained the solution in the ice-covered domain, the velocity potential ϕ, which exists in the free-surface domain, is provided by the integral representation (Eq. 15a). In this equation we may use the now-known values of the velocity potential and its radial derivative on the ice edge, which we have produced in the form of a Fourier series, where the weight of each mode is given by the appropriate entry of either $\mathbf{f}_0$ or $\mathbf{f}_1$. Hence the solution within the entire channel is known and may be reproduced with the necessary phase change to give the representation for the infinite domain.

NUMERICAL RESULTS

Here we give some numerical results for example problems, and we restrict our attention to the single channel Ω in which our calculations are made, and the solitary floe that exists in it. We concentrate on the effects of the floe interactions, as well as the additional new features that are unique to this model of a varying ice thickness and Archimedean draught. Our figure uses the x-axis as its horizontal axis. Cross-sections of the displacement of the solitary floe in the channel are shown along the interval it occupies of the x-axis, together with the transmitted free-surface displacement in a vicinity of the floe. That is, we have removed the incident wave, which has been normalised to 1 m in amplitude, from the plots of the free-surface profile.

In each figure, comparisons are made of the flexure of the individual floe and corresponding free-surface profile when a particular parameter is varied. The bed depth, which is of secondary importance in our considerations, is set as $h = 20$ m throughout. Also, for the remainder of this work we will use the frequency $\omega = 1$ rad/s, which gives an incident wavelength of approximately 60 m. As the length of the incident wave becomes shorter with respect to the dimensions of the floes, a greater proportion of the wave energy will be reflected by the array, and more interactions between the floes will occur. Here we have chosen a physically realistic value for the incident wave but also one that is capable of producing floe-floe interactions and hence results of interest.

Fig. 2 displays 4 separate cases of scattering, comparing the effects of floe separation $y_1 = 2(y_0 - R)$, with $y_1 = 5$ m, 10 m, 40 m and 100 m. In each case the floe is of radius $R = 50$ m, uniform thickness $D = 1$ m and zero draught, and the incident wave propagates at an angle of $\vartheta = \pi/6 \equiv 30°$.

Significant flexure of the floe in Ω is evident for all of the separation distances, with amplitudes of 0.25∼0.5 m. Further, we see in all 4 floe profiles that the dominant wavelengths, which are comparable to the length of the floe, appear to be approximately equal. The results shown are snapshots of the floes at the same instant in time ($t = 0$), and in all cases the displacements of the floes are extremely similar qualitatively and quantitatively, but they are not identical. Hence we infer that the floe separation has some, but only a little, effect on the ice flexure. This effect would diminish to negligible amounts if we were to increase the separation.

For the free-surface profiles, we first note the size of the waves present, with amplitudes of up to 2 m close to the floe, although these will settle to values below 1 once they have reached a sufficient distance from the array. This indicates that the majority of the wave energy propagates through the array of floes. The shape of the free surface in the vicinity of the ice edge becomes more

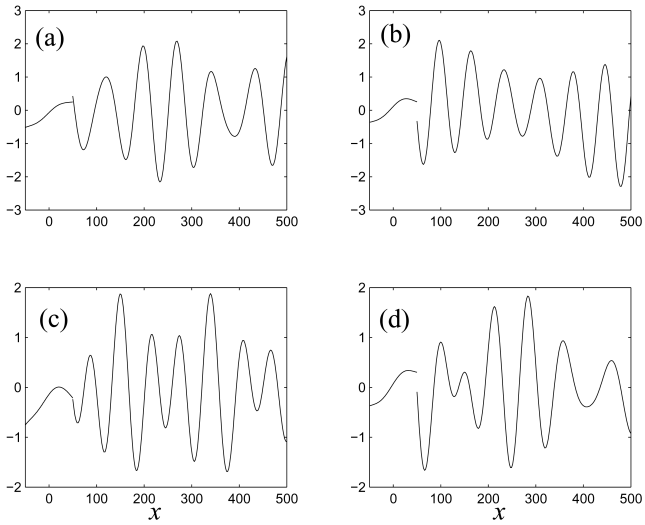

Fig. 2 Cross-sections of floe displacement and transmitted wave. Uniform floes of radius $R = 50$ m, thickness $D = 1$ m and zero draught, with separations: (a) $y_1 = 5$ m, (b) 10 m, (c) 40 m, and (d) 100 m. Incident wave of frequency $\omega = 1$ rad/s and angle $\vartheta = \pi/6$.

complicated as the separation increases, which may be attributed to the greater excitation of waves at angles other than that of the incident wave when there is more space between the floes.

In Fig. 3 we investigate the influence of introducing an Archimedean draught to the scattering process. The 2 uniform thicknesses $D = 1$ m and 2 m are chosen for the floes, with the results for the zero-draught floes, $d = 0$, given by the solid curves and the floes with an Archimedean draught, $d = \rho_i/\rho_w = 0.9$ m or 1.8 m, respectively, given by the dotted curves. Shown are 3 floe radii—$R = 25$ m, 50 m and 100 m—along with the corresponding free-surface profile in each case. The separation of the floes is set as $y_1 = 5$ m, and the incoming wave is normally incident.

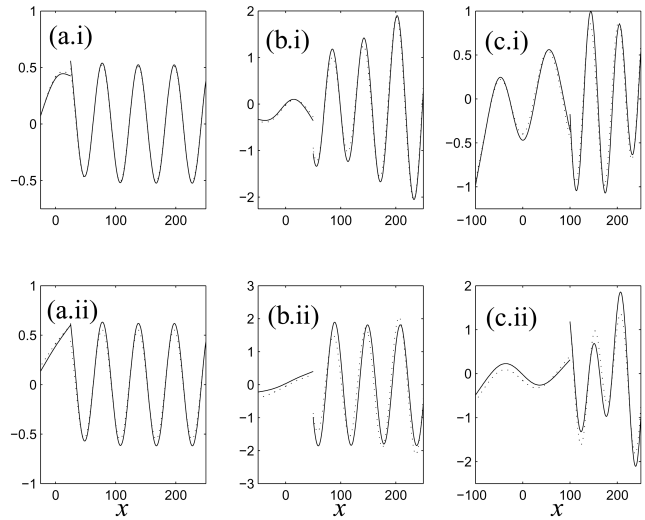

Fig. 3 Cross-sections of floe displacement and transmitted wave. Uniform floes of radius (a.i-ii) $R = 25$ m, (b.i-ii) $R = 50$ m and (c.i-ii) $R = 100$ m, separation $y_1 = 5$ m, and thickness $D = 1$ m in parts (i) and $D = 2$ m in parts (ii). Solid lines = zero-draught; dotted lines = Archimedean draught. Incident wave of frequency $\omega = 1$ and angle $\vartheta = 0$.

The introduction of realistic submergence is clearly visible in the flexure of the floes and becomes more evident as the breadth of each floe in the array increases. We note, however, that the qualitative and quantitative properties of the corresponding floes are consistent. As may be anticipated, differences between the corresponding zero-draught and Archimedean-draught floes increase as the thickness gets larger. Thus the 2 profiles are most distinct when $R = 100$ m and $D = 2$ m. Accordingly, we note similar differences between the transmitted free-surface profiles generated by the zero-draught and Archimedean-draught floes. We thus conclude that, for the chosen parameters, an Archimedean draught is important in relation to the displacement of the floes and the scattered wave for relatively wide and thick floes.

We again note that we expect the accuracy of our single-mode approximation (Eq. 6) to diminish somewhat as the thickness and draught of the floes become greater. In these cases the effects of the evanescent waves are more significant. However, we still expect that our results will reproduce the characteristics of the full-linear solution, and that our findings are representative of the situation being modelled.

Fig. 4 shows the investigation of the effects of adding surface undulations on the floes; results for arrays with 3 different choices of shape of floe are shown. All are of radius $R = 50$ m and share the same mass. One shape of floe is that of the uniform thickness $D = 1$ m; the remaining 2 have quadratic variations in their upper and lower surfaces in the ratio 2:7 (sail:keel). For one, the variations are convex, so that the middle of the floe is thicker than the edge of the floe, at which point $D = 0.7$ m. On the final floe the variations are concave, and it is thinner at its centre than at its edge; this floe has an edge thickness of $D = 1.3$ m.

In order to calculate the results for varying ice thicknesses, we are required to impose a disc around the centre of the floe of arbitrarily small radius ϵ, within which the geometry is uniform. As alluded to earlier, for the 2 varying floes used in this figure, progressively smaller values of ϵ were taken to ensure convergence, and for the presented results $\epsilon = 1$ m. However, it was found that a much larger value of ϵ for the radius, say $\epsilon = 10$ m, would give nearly identical results.

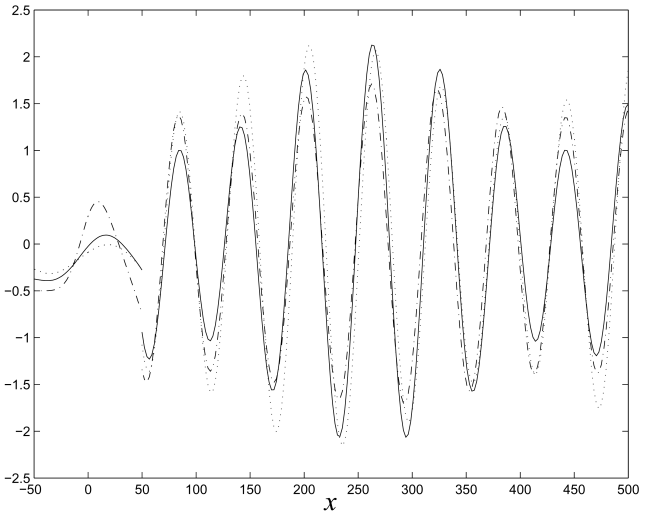

Fig. 4 Cross-sections of floe displacement and transmitted wave. Floes are of radius $R = 50$ m and mass $2500\pi\rho_i$ kg, with separations of $y_1 = 5$ m. Solid line is uniform floe $D = 1$ m. Broken lines are floes with quadratic variations in sail:keel ratio 2:7, with $D = 0.7$ m (dotted) at $r = R$ and $D = 1.3$ m (dot-dash) at $r = R$. Incident wave of frequency $\omega = 1$ and angle $\vartheta = 0$.

The results show that the flexure of the convex floe is similar to the uniform floe, with little more than a downward transition. However, the displacement of the concave floe is markedly different from the other 2. It is particularly notable for this floe that, as the wave passes through, it grows in amplitude. The transmitted waves generated in all 3 cases closely resemble one another in shape and amplitude, but with some phase change evident, especially for the concave floe.

CONCLUSIONS

During this work we have set out a means for calculating a low-cost approximation to the scattering of a plane wave by an infinite straight-line array of floes. We allowed these floes to vary in thickness as well as possess a realistic draught. Such a model can be considered a representation of the bands of ice floes that form at the edge of the MIZ. It also presents the basis for investigating multiple straight-line arrays, which may be used to model other, more prominent MIZ regions.

In order to solve the problem, we made the assumption that each floe is considered identical and equispaced. A restriction of axisymmetry was also placed on the floes. Because the remaining problem was periodic, it could be solved by considering a single channel, containing a solitary floe. For simplicity, we chose to apply an approximation of the vertical dependence of the solution by the single-mode that supports propagating waves. Application of a variational principle then reduced the calculation to the horizontal plane alone.

By using a Fourier decomposition of the azimuthal motion of the unknown functions, it was possible to form an ODE set in the radial coordinate within the ice-covered domain. A suitable Green's function was derived for the free-surface domain, which was applied, in conjuction with Green's theorem, to provide the necessary boundary data along the ice edge. Knowledge of the solution at the ice edge then gave the solution in the free-surface domain through an integral expression.

Numerical results were given for a number of example problems in which we investigated the displacement of the floe and the transmission of the incident wave through the array into the opposing free-surface domain. In one set of results it was found that, for our restricted set of parameters, the floe separation has a minimal but visible influence on the flexure of the floes making up the array, for floes of a 50-m radius in the separation range between 5 m and 100 m. In the free surface, the transmitted wave became more complex in a vicinity of the floes as the separation distance was increased. In the second set of results we noted that the introduction of an Archimedean draught had a noticeable effect on the properties of the flexural-gravity wave travelling through the ice, especially for larger floes, and an equivalent influence on the transmitted waves. The final set of results compared 3 floes of an identical mass and radius, but in which 2 contained surface undulations, one convex and the other concave. For these floes, the profile generated by the convex floe differed minimally from those of the uniform floe, although the concave floe displayed prominent differences.

ACKNOWLEDGEMENTS

Supported by the University of Otago and by the Marsden Fund Council from Government funding administered by the Royal Society of New Zealand.

REFERENCES

Abramowitz, M, and Stegun, I (1964). *Handbook of Mathematical Functions*, Dover.

Andrianov, AI, and Hermans, AJ (2005). "Hydroelasticity of a Circular Plate on Water of Finite or Infinite Depth," *J Fluid Struct*, Vol 20, No 5, pp 719–733.

Bauer, J, and Martin, S (1980). "Field Observations of the Bering Sea Ice Edge Properties During March 1979," *Monthly Weather Rev*, Vol 108, pp 2045–2056.

Bennetts, LG (2007). "Wave Scattering by Ice Sheets of Varying Thickness," *PhD Thesis*, Univ of Reading, UK.

Bennetts, LG, Biggs, NRT, and Porter, D (2007). "A Multi-mode Approximation to Wave Scattering by Ice Sheets of Varying Thickness," *J Fluid Mech*, Vol 579, pp 413–443.

Bennetts, LG, Biggs, NRT, and Porter, D (2008). "Wave Scattering by an Axisymmetric Ice Floe of Varying Thickness," *IMA J Appl Math*, doi: 10.1093/imamat/hxn019.

Meylan, M (2002). "Wave Response of an Ice Floe of Arbitrary Geometry," *J Geophys Res*, Vol 107, doi:10.1029/200JC00713.

Meylan, M, and Squire, VA (1996). "Response of a Circular Ice Floe to Ocean Waves," *J Geophys Res*, Vol 101, pp 8869–8884.

Peter, MA, and Meylan, M (2004). "Infinite Depth Interaction Theory for Arbitrary Floating Bodies Applied to Wave Forcing of Ice Floes," *J Fluid Mech*, Vol 500, pp 145–167.

Peter, MA, Meylan, M, and Chung, H (2004). "Wave-scattering by a Circular Elastic Plate in Water of Finite Depth: A Closed Form Solution," *Int J Offshore and Polar Eng*, ISOPE, Vol 14, No 2, pp 81–85.

Peter, MA, Meylan, M, and Linton, CM (2006). "Water-Wave Scattering by a Periodic Array of Arbitrary Bodies," *J Fluid Mech*, Vol 548, pp 237–256.

Porter, D, and Porter, R (2004). "Approximations to Wave Scattering by an Ice Sheet of Variable Thickness over Undulating Topography," *J Fluid Mech*, Vol 509, pp 145–179.

Timoshenko, S, and Woinowsky-Krieger, S (1959). *Theory of Plates and Shells*, 2nd ed, McGraw-Hill.

Wang, CD, Meylan, MH, and Porter, R (2007). "The Linear Wave Response of a Periodic Array of Floating Elastic Plates," *J Eng Math*, Vol 57, No 1, pp 23–40.